4 Techniques for Characterizing Lignin

Nicole M. Stark, Daniel J. Yelle and Umesh P. Agarwal
USDA Forest Service, Forest Products Laboratory, One Gifford Pinchot Drive, Madison, WI, USA

OUTLINE

1. Introduction

Many techniques are available to characterize lignin. The techniques presented in this chapter are considered nondegradative, which are commonly applied to lignin. A brief discussion of lignin structure is included with this chapter to aid the reader in understanding why the discussed characterization techniques are appropriate for the study of lignin. Because the chemical structure and composition of lignin vary from source, type of lignin, and isolation method, as discussed in the preceding chapters, characterization is important. Obtaining the molecular weight of a lignin sample can give information, such as degree of polymerization, even before investigating the chemical structure. Chemical structure characterization is most often accomplished using spectroscopic methods. Understanding the chemical structure can be useful in determining lignin sources, degradation of lignin samples, relationship between physical properties and thermal properties, selecting appropriate modification methods, and determining the efficacy of modifications. Chemical structure characterization techniques discussed in this chapter include ultraviolet (UV) spectroscopy, Fourier-transform infrared (FTIR) spectroscopy, Raman spectroscopy, nuclear magnetic resonance (NMR) spectroscopy, and X-ray photoelectron spectroscopy (XPS). Physical properties such as thermal and mechanical properties can be related back to the chemical structure. Differential scanning calorimetry (DSC) and thermogravimetric analysis (TGA) are often employed during the investigation of thermal properties of lignin, while dynamic mechanical analysis (DMA) can be used to investigate both thermal and mechanical properties. In each section, a brief introduction to each technique is followed by examples of its application to lignin. Finally, the reader is directed toward select resources that are available for a more complete understanding of these methods, and their applicability to lignin.

2. Lignin Structure

Lignin, comprising roughly 15% of all terrestrial biomass, is one of the most recalcitrant of all natural polymers. It is made up of chemical combinatorial, stereoirregular linkages, which are formed in the cell walls of vascular plants via free radical coupling reactions between various 4-hydroxycinnamyl alcohols and the growing polymer as an "*endwise*

Lignin in Polymer Composites. http://dx.doi.org/10.1016/B978-0-323-35565-0.00004-7

polymerization" (Boerjan et al., 2003). These precursor alcohols, coined monolignols, include coniferyl alcohol (G lignin), sinapyl alcohol (S lignin), and *p*-coumaryl alcohol (H lignin) (Figure 1). During lignin biosynthesis, these monolignols are translocated across the plasma membrane via transporters, but much of this mechanism remains a mystery (Ehlting et al., 2005). The radical form of each monolignol prefers to couple at their β-positions, creating mostly β−O−4, β−β, and β−5 dimers (Figure 2). Endwise coupling, adding one monomeric radical at a time, results in a highly complex polymer (Figure 3). Although the proposed lignin structures do not represent a precise molecular structure, because the exact structure remains elusive, lignin can be characterized using a variety of techniques.

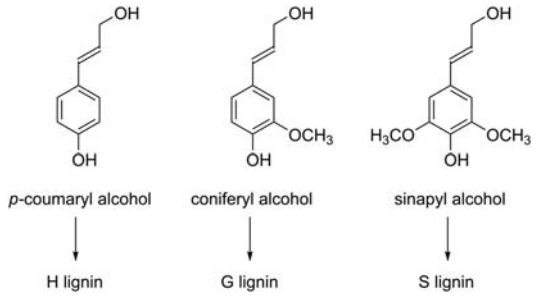

Figure 1 Lignin precursors: *p*-coumaryl alcohol (H lignin), sinapyl alcohol (S lignin), and coniferyl alcohol (G lignin).

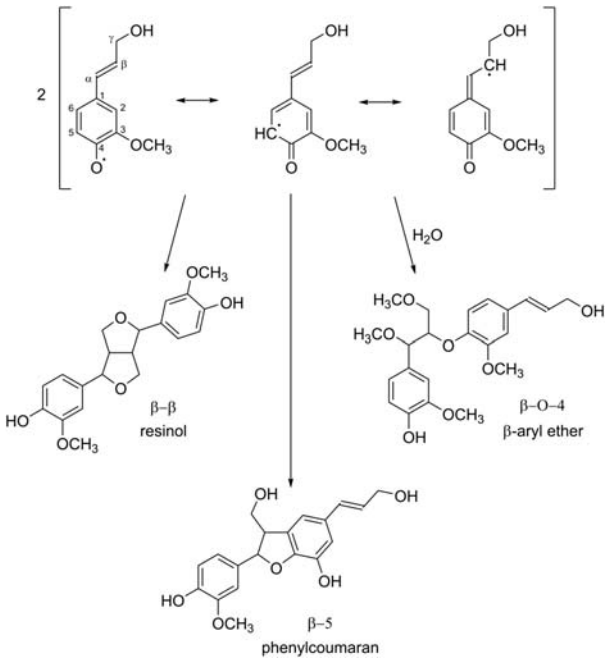

Figure 2 Resonance-stabilized dimerization of two dehydrogenated coniferyl alcohol monomers produce mainly β-aryl ether (β−O−4), resinol (β−β), and phenylcoumaran (β−5) linkages (Adapted from Vanholme et al., 2010).

In lignocellulosic materials, lignin can be thought of as the matrix that holds cellulose fibers together. It is a brittle, relatively inert material that acts as both a bonding agent and stiffening agent. During cell wall biosynthesis, lignification of the fiber cell wall increases stiffness and allows stress transfer between the hemicellulose matrix and cellulose. Generally softwoods have a larger percentage of lignin than hardwoods, accounting for 23−33% in softwoods and 16−25% in hardwoods, respectively (Fengel and Wegener, 1983). Lignins found in softwoods and hardwoods can be characterized based on the amount of each type of lignin present. Softwoods generally have a much higher percentage of G lignin. For example, the G:S:H ratio for loblolly pine (*Pinus taeda*) is 86:2:13 (Fengel and Wegener, 1983). Hardwoods are primarily composed of guaiacyl and syringyl precursors. The S lignin content of hardwood can vary between 20% and 60% (Fengel and Wegener, 1983).

3. Molecular Weight

The molecular weight distribution can be determined using high-performance liquid chromatography. This technique involves introducing a sample mixture into a column. The sample percolates through the column filled with sorbents, and the components move through at different velocities depending upon its chemical nature. The retention time, or the time at which the sample emerges from the column, is measured. Elution can be measured using light scattering (LS), UV absorbance, or refractive index (dRI). This technique is readily applied to lignin dissolved in a solvent.

Figure 4 shows the molecular weight distributions of kraft lignin (KL) from ponderosa pine (*Pinus ponderosa*). In this case, elution was measured using LS, UV absorbance at 280 nm (UV), and dRI. All three curves were normalized at 1. This figure shows that the lignin had a normal curve with a small fraction of low-molecular weight oligomers. Using the LS curves, weight-average molecular weight (M_w), number-average molecular weight (M_n), and polydispersity (M_w/M_n) of the lignin are

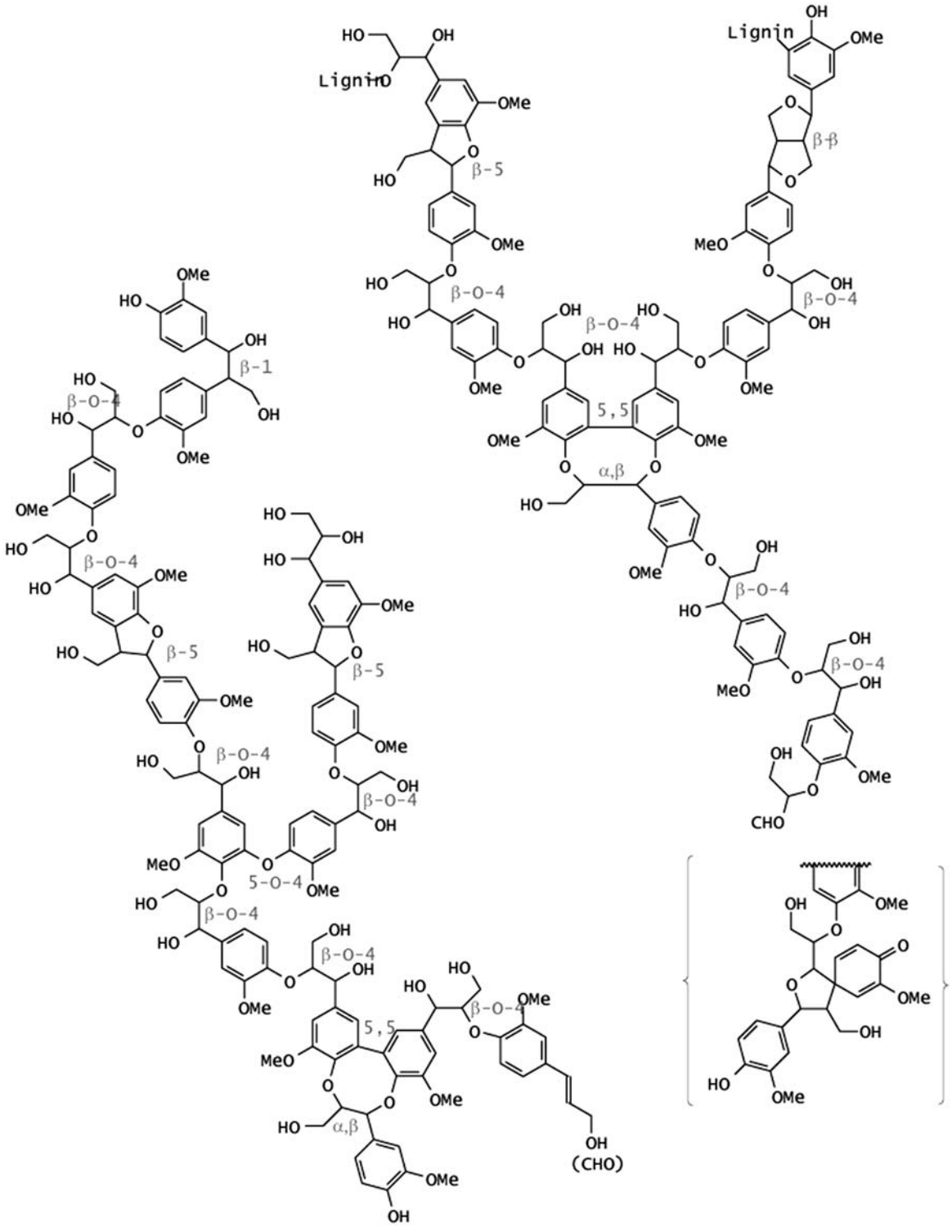

Figure 3 Representative molecular structure of softwood lignin. Interunit linkages are annotated (Agarwal and Reiner, 2009).

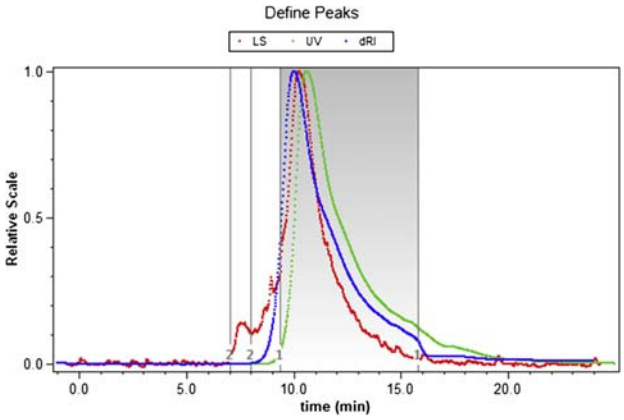

Figure 4 Elution time for a CO_2 precipitated kraft lignin detected using light scattering (LS), ultraviolet absorbance (UV), and refractive index (dRI).

Table 1 Reported Precipitated CO_2 Kraft Lignin Molecular Weight Values for Two Areas of the Elution Curve Measured by Light Scattering

	Peak 1	Peak 2
M_w	9.090×10^7	4.490×10^7
M_n	7.946×10^4	3.817×10^7
M_w/M_n	1.144	1.176

reported (Table 1). In this case, the sample lignin had a high M_w and a low polydispersity. This indicates a relatively pure sample of lignin.

4. Chemical Structure Characterization

Lignin is a complex polymer, and many techniques have been used to determine its chemical structure. The chemical structure can vary based on source, type, and isolation method and therefore, a large number of chemical structure characterization techniques are used to identify these differences. Lignin is also routinely modified for various reasons. Structural characterization can also be used to identify appropriate modification to lignin and to investigate the effectiveness of the modification. The following spectroscopic methods are routinely employed in the study of lignin.

4.1 UV Spectroscopy

UV spectroscopy refers to absorption spectroscopy in the UV region (200–400 nm). In practice, a spectrophotometer measures the intensity of light passing through a sample (I) and compares it to the intensity of light before it passes through the samples (I_o). The ratio I/I_o is called the transmittance and reported as (%T). The absorbance, A, is calculated based on transmittance ($A = -\log(\%T/100\%)$). To record transmittance samples are placed in a UV–Vis spectrophotometer. Samples are most often liquids; therefore lignin is typically dissolved in a solvent. Because this is a simple method, UV spectrophotometric investigations are commonly used to characterize lignin. However, care must be taken in selecting the appropriate solvent, as the spectrum may be modified due to solvent effects. Potential solvents include water, dimethylformamide, ethanol, 2-methoxyethanol, dioxane, dimethylsulfoxide (DMSO), pyridine, dicholoroethane, cellosolve, and hexafluoropropanol (Baeza and Freer, 2001). Of these, hexafluoropropanol has been identified as suitable for analysis of lignins for both UV and IR spectroscopy. The solvent has high UV transmittance properties without interference from the degradation products of polysaccharides (Wegener et al., 1983). The aromatic nature of lignin

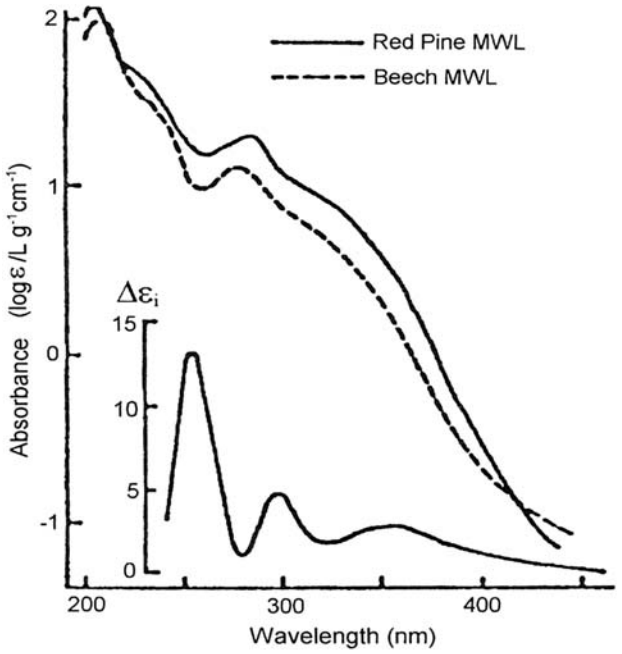

Figure 5 UV and $\Delta\varepsilon_i$ spectra of red pine and beech milled wood lignins (MWLs) (Baeza and Freer, 2001).

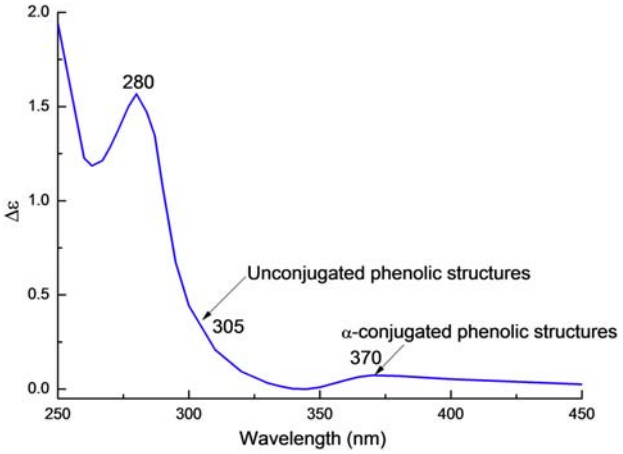

Figure 6 Ionization spectrum ($\Delta\varepsilon_i$) of a kraft wood lignin from ponderosa pine.

results in a strong absorption in the UV region. In Figure 5, strong bands appear at 205 and 280 nm. The band at 280 nm is the result of a benzene ring substituted by hydroxyl or methoxyl groups (Sakibara and Sano, 2001).

In alkaline solutions, phenolic hydroxyl groups are ionized and the absorption changes toward longer wavelengths and higher intensities. Therefore, it is useful to examine the ionization spectrum ($\Delta\varepsilon_i$), the spectrum derived from a neutral solution subtracted from the spectrum derived from an alkaline solution. The ionization spectrum is commonly used to determine the phenolic hydroxyl groups in lignin preparation (Goldschmid, 1954). The ionization spectrum for KL (Figure 6) can be used to determine the phenolic group content. The 300 nm contribution of the difference curve is characteristic of phenolic hydroxyl groups without conjugation. The maximum at 370 nm is characteristic of conjugated phenolic structures.

4.2 FTIR Spectroscopy

IR spectroscopy is an absorption technique made possible because molecular vibration modes absorb specific frequencies of the electromagnetic spectrum at varying intensities. However, a change in electric dipole moment must occur during the vibration. During IR spectroscopy electromagnetic radiation in the IR region is either transmitted through the sample or reflected off the surface. IR photons which match the resonant mode frequencies in the molecules are absorbed. The radiation emitted in the IR region is recorded, and the frequencies not present are noted. FTIR spectroscopy allows for the spectra to be recorded. The radiation emitted in the IR region is also referred to in terms of wave numbers (υ), which is the number of waves per centimeter. Characterization of lignin is commonly conducted in the mid-IR region, which corresponds to electromagnetic radiation with wavenumbers between 4000 and 400 cm^{-1}. Penetration of the IR beam into the sample is very small; therefore FTIR spectroscopy is a powerful method for determining functional groups present only at the surface of a sample.

There are several techniques that can be employed to obtain FTIR spectra. Attenuated total reflectance (ATR) is a method that directly analyzes a sample and no sampling method is needed. In ATR-FTIR, there is an intimate contact between the sample surface to be analyzed and a crystal. The beam travels through the crystal and excites the surface of the sample. The wavelengths of the photons emitted by the sample are recorded. Another technique is diffuse reflectance infrared Fourier transform (DRIFT) spectroscopy. DRIFT spectroscopy is useful for characterizing powders. The powder is typically mixed with a purified salt and pressed to form a translucent pellet through which the passing infrared beam. Both of these techniques are commonly applied to the characterization of lignin because the sample can be analyzed quickly, with minimal preparation, and only small amounts are needed. Table 2 summarizes the assignment of common absorption bands in softwoods and hardwoods (Agarwal and Atalla, 2010).

Figure 7 shows a representative FTIR spectrum of KL derived from a softwood (*P. ponderosa*). The broad peak at 3409 cm^{-1} is assigned to OH stretching. Other strong bands include those at 1594 cm^{-1} (symmetric aryl ring stretching), 1512 cm^{-1} (asymmetric aryl ring stretching), 1463 cm^{-1} (asymmetric CeH deformation) 1266 cm^{-1} (aryl ring breathing), and 1030 cm^{-1} (aromatic CH in plane deformation).

4.3 Raman Spectroscopy

Raman spectroscopy is similar to IR spectroscopy in that an incident IR beam will make contact with the sample. However, rather than reporting the absorption of the photons as a specific frequency, the photon frequency shifts. The shift is a result of the Raman effect or inelastic LS. As the sample is irradiated by a laser beam, it is excited. The difference in energy between the original state and the post-excitation ground state shifts the photon's frequency

Table 2 Assignment of Bands in FTIR Spectra of Softwood and Hardwood Milled Wood Lignins (MWLs)

Softwood[a,c] (cm^{-1})		Hardwood[b,c] (cm^{-1})		Assignment
3430	vs	3440	vs	O–H stretch, H-bonded
2938	m	2942	m	C–H stretch methyl and methylene groups
2885	sh	2882	sh	C–H stretch in methyl and methylene groups
2849	sh	2848	sh	C–H stretch O–CH_3 group
1717	sh	1737	vs	C═O stretch, unconjugated ketone, carboxyl, and ester groups
1667	sh	1670	sh	Ring-conjugated C═O stretch of coniferaldehyde/sinapaldehyde
1645	sh	1643	sh	Ring-conjugated C═C stretch of coniferyl/sinapyl alcohol
1600	s	1596	s	Aryl ring stretching, symmetric
1513	vs	1506	vs	Aryl ring stretch, asymmetric
1466	s	1464	s	C–H deformation, asymmetric
1458	sh	1425	m	O–CH_3 C–H deformation, asymmetric
1428	m	1379	m	Aromatic skeletal vibration combined with C–H in plane deformation
1375	w	1367	sh	O–CH_3 C–H deformation symmetric
1331	sh	1330	m	Aryl ring breathing with C–O stretch
1270	vs	1252	vs	Aryl ring breathing with C═O stretch
1226	m			C–C, C–O, and C═O stretches
1142	s	1159	sh	Aromatic C–H in plane deformation
		1127	vs	Aromatic C–H in plane deformation
1085	w	1082	sh	C–O deformation, secondary alcohol, and aliphatic ether
1035	s	1050	vs	Aromatic C–H in plane deformation
914	vw	905	w	C–H deformation of out of plane, aromatic ring
878	sh			C–H deformation of out of plane, aromatic ring
863	w			C–H deformation of out of plane, aromatic ring
823	w			C–H deformation of out of plane, aromatic ring
748	vw			CCH wag
742	vw			Skeletal deformation of aromatic rings, substituent side groups, side chains

[a]*Black spruce milled wood lignin, guaiacyl lignin.*
[b]*Aspen milled wood lignin, guaiacyl and syringyl lignin.*
[c]*vs very strong; s strong; m medium; w weak; vw very weak; sh shoulder; relative to other peaks in the spectrum.*
Adapted from Agarwal and Atalla (2010).

away from the excitation wavelength. There are well-defined frequencies at which the vibration modes scatter.

Raman instruments are either a dispersive type (Long, 1977; Freeman, 1974) or are based on an interferometer (Hendra et al., 1991). A dispersive instrument consists of a source of monochromatic radiation (laser), an appropriate way of sampling, suitable gratings (for dispersion of the scattered radiation), and a detection device. In a dispersive Raman spectrometer, a detector consists of either a photomultiplier tube or some multichannel device (e.g., charge-coupled device or photodiode array). A multichannel detector is particularly useful where high resolution is not necessary and rapid analysis is desired (Agarwal and Atalla, 2010).

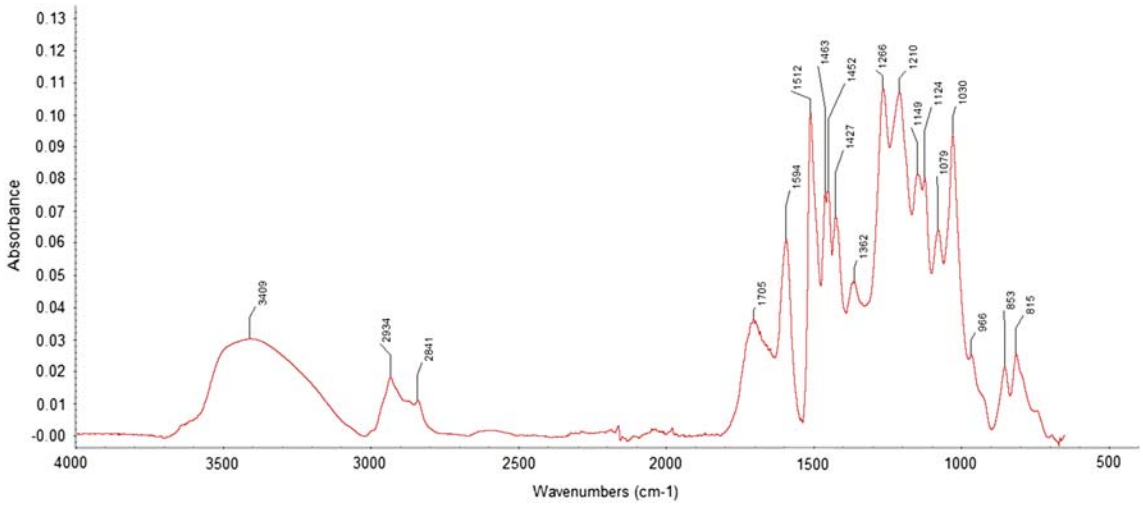

Figure 7 Fourier-transform infrared spectra of a softwood kraft lignin derived from ponderosa pine.

Raman spectroscopy is most often conducted using visible lasers; however, near-IR laser-based Raman spectroscopy has been particularly useful in the study of lignins. Table 3 summarizes the assignment of bands in FT-Raman spectra.

Two special Raman techniques important for the analysis of lignin include micro-Raman and Raman imaging (Agarwal and Atalla, 2010). Micro-Raman couples an optical microscope to a Raman spectrometer. This allows for analysis at a specific

Table 3 Assignment of Bands in FT-Raman Spectra of Softwood and Hardwood Milled Wood Lignins (MWLs)

Softwood[a,c] (cm^{-1})		Hardwood[b,c] (cm^{-1})		Assignment
3071	m	3068	m	Aromatic C–H stretch
3008	sh	3003	sh	C–H stretch in OCH_3, asymmetric
2940	m	2939	s	C–H stretch in O–CH_3, asymmetric
2890	sh	2893	sh	C–H stretch in R_3C–H
2845	m	2847	sh	C–H stretch in OCH_3, symmetric
1662	s	1661	s	Ring-conjugated C═C stretch of coniferyl/sinypl alcohol; C═O stretch of coniferaldehyde/sinapaldehyde
1621	sh	1620	sh	Ring-conjugated C═C stretch of coniferaldehyde/sinapaldehyde
1597	vs	1595	vs	Aryl ring stretching, symmetric
1508	vw	1501	vw	Aryl ring stretch, asymmetric
1453	m	1455	s	O–CH_3 deformation; CH_2 scissoring; guaiacyl/syringyl ring vibration
1430	w	1426	w	O–CH_3 deformation; CH_2 scissoring; guaiacyl/syringyl ring vibration
1392	sh	1395	sh	Phenolic O–H bend
1363	sh	1367	sh	C–H bend in R_3C–H
1334	m	1331	s	Aliphatic O–H bend
1298	sh			Aryl–O of aryl–OH and aryl–O–CH_3; C═C stretch of coniferyl alcohol
1272	m	1272	m	Aryl–O of aryl–OH and aryl–O–CH_3; guaiacyl/syringyl ring mode

(*Continued*)

Table 3 Assignment of Bands in FT-Raman Spectra of Softwood and Hardwood Milled Wood Lignins (MWLs) (*Continued*)

Softwood[a,c] (cm^{-1})		Hardwood[b,c] (cm^{-1})		Assignment
1226	vw	1224	w	Aryl–O of aryl–OH and aryl–O–CH_3; guaiacyl/syringyl ring mode
1192	w	1190	w	A phenol mode
		1156	sh	Unassigned
1136	m	1130	m	A mode of coniferaldehyde/sinapaldehyde
1089	w	1088	w	Out of phase C–C–O stretch of phenol
1033	w	1037	m	C–O of aryl–O–CH_3 and aryl–OH
975	vw	984	sh	CCH and –HC═CH– deformation
928	vw	918	sh	CCH wag
895	vw	899	w	Skeletal deformation of aromatic rings, substituent side groups, side chains
787	w	797	w	Skeletal deformation of aromatic rings, substituent side groups, side chains
731	w	727	w	Skeletal deformation of aromatic rings, substituent side groups, side chains
637	vw	638	w	Skeletal deformation of aromatic rings, substituent side groups, side chains
		597	m	Skeletal deformation of aromatic rings, substituent side groups, side chains
588	vw	588	w	Skeletal deformation of aromatic rings, substituent side groups, side chains
557	vw			Skeletal deformation of aromatic rings, substituent side groups, side chains
534	vw	531	m	Skeletal deformation of aromatic rings, substituent side groups, side chains
		522	sh	Skeletal deformation of aromatic rings, substituent side groups, side chains
		503	vw	Skeletal deformation of aromatic rings, substituent side groups, side chains
491	vw	490	vw	Skeletal deformation of aromatic rings, substituent side groups, side chains
		472	vw	Skeletal deformation of aromatic rings, substituent side groups, side chains
457	vw	461	vw	Skeletal deformation of aromatic rings, substituent side groups, side chains
		447	vw	Skeletal deformation of aromatic rings, substituent side groups, side chains
		431	vw	Skeletal deformation of aromatic rings, substituent side groups, side chains
		417	vw	Skeletal deformation of aromatic rings, substituent side groups, side chains
384	w			Skeletal deformation of aromatic rings, substituent side groups, side chains
361	w	369	m	Skeletal deformation of aromatic rings, substituent side groups, side chains

[a]*Black spruce milled wood lignin, guaiacyl lignin.*
[b]*Aspen milled wood lignin, guaiacyl and syringyl lignin.*
[c]*vs very strong; s strong; m medium; w weak; vw very weak; sh shoulder; relative to other peaks in the spectrum.*
Adapted from Agarwal and Atalla (2010).

location on a nonheterogeneous sample. In Raman imaging, a spatially resolved image is produced either as a line map using a single-element detector or as a 2D map using multichannel detectors.

FT-Raman spectra of black spruce and aspen milled wood (MW) lignins are shown in Figure 8. One can see characteristic peaks at 3068 cm^{-1} (aromatic C−H stretch), 2939 cm^{-1} (asymmetric C−H stretch in OCH_3), 1661 cm^{-1} (ring-conjugated C═C stretch; C═O stretch), 1595 cm^{-1} (symmetric aryl ring stretching), and 1331 cm^{-1} (aliphatic O−H bend). FT-Raman spectroscopy is particularly useful for the study of lignins because spectra with minimum contribution of autofluorescence can be obtained. Using this technique, it was found that no significant differences existed between the FT-Raman spectra

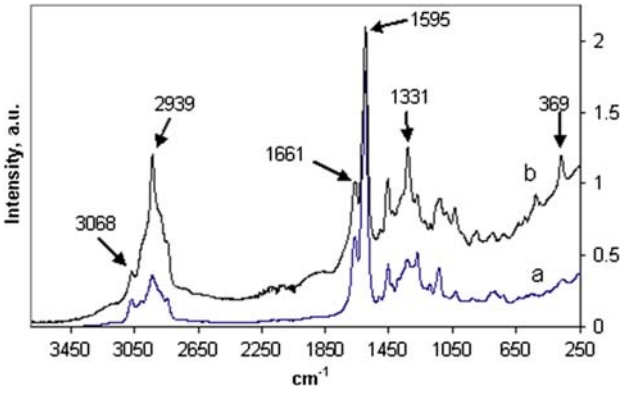

Figure 8 FT-Raman spectra of (a) black spruce and (b) aspen milled wood lignins (Agarwal and Atalla, 2010).

of native and MW lignin from black spruce (Agarwal and Ralph, 1997). Therefore an MW lignin spectrum can be considered to represent a native lignin spectrum.

4.4 NMR Spectroscopy

NMR spectroscopy can be defined as an indispensable tool which applies a magnetic field to an atomic nucleus (e.g., the most common stable isotopes ^{1}H, ^{13}C, ^{15}N) and radio frequency pulses to characterize the resonant frequency of that atomic nucleus according to its chemical or environmental surroundings. As each nucleus is perturbed from its original equilibrium state, that nucleus will display a characteristic decay signal back to equilibrium and this signal is like an encrypted map of the chemical structure of molecules and polymers. The electrons of the atom circulate along the direction of the applied magnetic field, and this causes a small opposing magnetic field at the nucleus. Electron density around nuclei in a molecule varies according to the types of nuclei and bonds it has, making the static and opposing magnetic fields differ. This phenomenon is called "chemical shift" (ppm or Hz) and is the fundamental piece of information used to characterize the structure of the molecule or polymer. Nuclei that are close to each other (i.e., 3 or less bond lengths apart) exert an influence on each other's opposing magnetic field, called "spin−spin coupling," allowing further elucidation of the interrelationships between protons in the molecule or polymer.

Historically, polymers, like that of lignin, presented a particular challenge for NMR studies. The higher molecular weight, greater viscosity, and lower solubility of polymers compared to small molecules makes for low mobility, leading to short relaxation times and broadening of signals and limiting a detailed characterization of polymeric components. A large portion of these issues can be circumvented by avoiding paramagnetic metals in workup and isolation of the plant sample, such as utilizing chelation techniques or milling the plant material in the absence of iron and oxygen. However, just as significant to the quality of the NMR spectrum is the lignin isolation methodology, the sensitivity of the instrument (e.g., magnet size, cryogenically cooled probe, etc.), and the acquisition parameters employed (Ralph and Landucci, 2010). No method yet exists that will allow for a complete characterization of lignin in its native state in the plant. Therefore, every lignin sample will have some variability from what first existed in nature.

Novel techniques now exist that attempt to eliminate the need for degradative isolation methods so that the lignin, as well as the polysaccharides, can be characterized in its most native state possible. Traditional analyses of plant cell wall lignin require fractionation, with the isolation of each component, to obtain qualitative and/or quantitative information about its composition and structure. However, component isolation procedures lead to alterations in native cell wall chemistry (via, e.g., deacylation, oxidation, or other degradative processes) (Lai and Sarkanen, 1971). It is now possible to analyze lignin polymers in ball-milled plant cell walls, without the need to separate the lignin from the polysaccharides (Lu and Ralph, 2003), with the caveat that ball milling will alter the lignin polymer structure to a certain degree based upon the milling conditions (Ikeda et al., 2002; Fujimoto et al., 2005). Through nondegradative dissolution of ball-milled wood cell wall material in DMSO and *N*-methylimidazole (NMI), and in situ acetylation, two-dimensional (2D) NMR can characterize lignin structures in considerable detail (Figure 9). Running this type of 2D NMR experiment called heteronuclear single-quantum coherence (HSQC), 1-bond ^{13}C-^{1}H correlation spectra in which carbons are directly correlated with their attached protons, shows that cell wall components separate out in the "contour map." The most intense peaks (black) are those of the cellulose carbons attached to their protons, which are surrounded by other unidentified polysaccharide components like hemicelluloses.

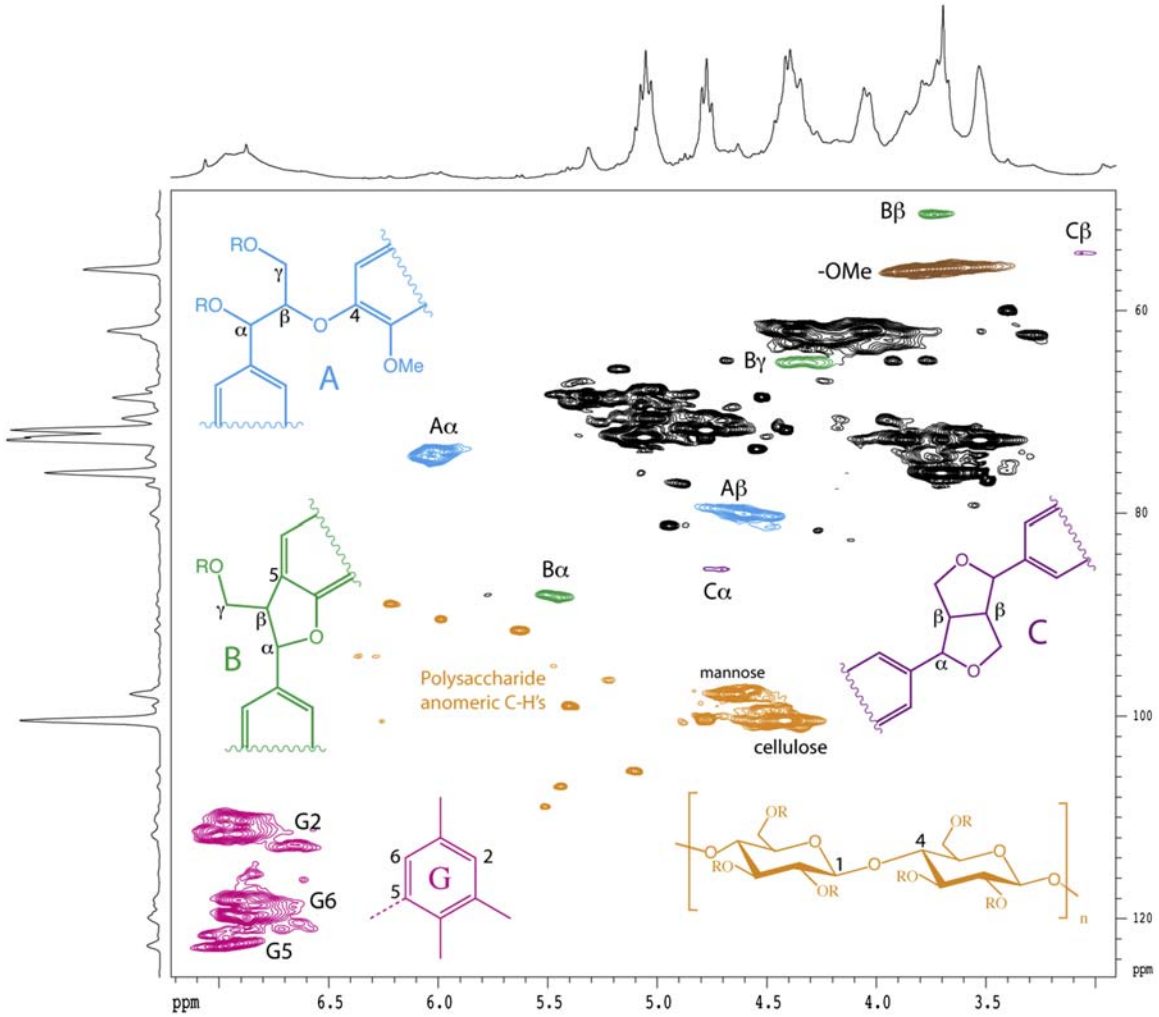

Figure 9 Two-dimensional $^{1}H-^{13}C$ correlation HSQC NMR spectrum of acetylated loblolly pine whole cell walls dissolved in chloroform at 360 MHz. Here the *x*-axis is proton and *y*-axis is carbon. This sample was ball milled using ZrO_2 ball bearings and cup for approximately 3 h (400 mg of wood). The following are included in the spectra: **A** (cyan, lighter gray in print versions) are β−O−4 units, **B** (green, light gray in print versions) are β−5 units, **C** (purple, black in print versions) are β−β units, **G** (magenta, dark gray in print versions) are the guaiacyl lignin aromatics, polysaccharide anomerics C−H (orange, lightest gray in print versions), and methoxyl from lignin (brown, gray in print versions). The black peaks are mostly aliphatics from polysaccharides (cellulose and hemicelluloses).

However, the anomeric C−H of cellulose and mannose can be seen as the large peaks in orange. The aromatic lignin region (magenta) shows all the C−H correlations found in the various guaiacyl (gymnosperm) units. Most of the lignin side chain units are well resolved. For example, the β-aryl ether (cyan) unit Aα and Aβ correlations are well resolved; however, the Aγ is hidden under the black polysaccharide region. Phenylcoumaran (β−5) units in green also are well resolved showing Bα, Bβ, and Bγ correlations. Other lignin units like resinol (β−β) and dibenzodioxocin (5−5/β−O−4) are present in the spectrum at lower contour levels due to their lower abundance. A more demanding experiment for acetylated cell wall material, and polymeric material in general, is the long-range ^{13}C-^{1}H correlation experiment called heteronuclear multiple-bond correlation (HMBC). This experiment is able to correlate a proton to a carbon that is two or three bonds away. It is a powerful experiment in that the connectivity of structural units can be identified. The challenge

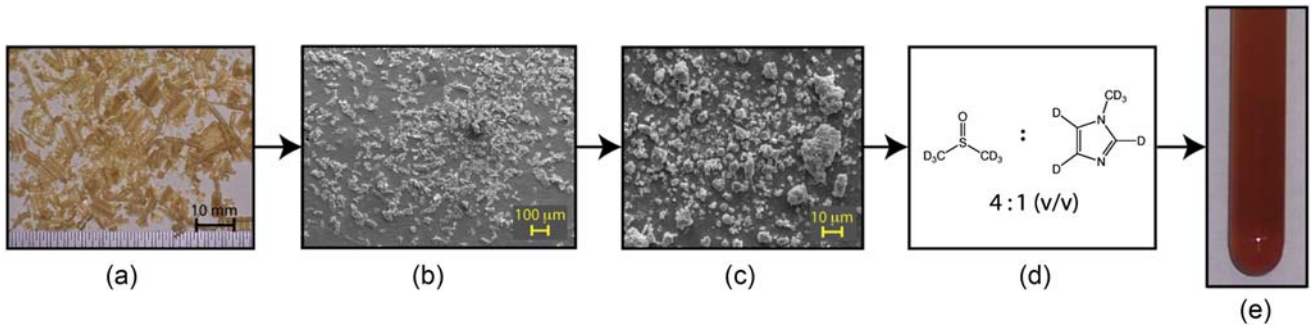

Figure 10 A diagram illustrating the nonderivatized dissolution of plant cell walls of *Pinus taeda*: (a) shavings produced via conventional jointer, (b) cryogenically mixer-milled shavings, (c) planetary ball-milled particles from the mixer mill, (d) dissolution method using DMSO-d_6 and NMI-d_6, (e) 5 mm NMR tube of pine cell walls in solution.

is that a delay of 80–100 ms is needed to allow for long-range coupling interactions to evolve. If the sample relaxes too quickly, as occurs with immobile polymers or metal-contaminated samples, the signal intensity is diminished.

Recently, utilizing the DMSO and NMI dissolution chemistry, wood and plant cell walls were characterized by 2D NMR in the perdeuterated solvents DMSO-d_6 and NMI-d_6 (Yelle et al., 2008a); Figure 10 describes the technique. This allowed characterization of the native chemistry of the cell wall, including natural acetates found on lignin syringyl units and acetyl side groups found acylating xylan and mannan units in hemicelluloses of *P. taeda*, *Populus tremuloides*, and *Hibiscus cannabinus* (Figure 11). In further simplified methods, DMSO-d_6 alone or DMSO-d_6/pyridine-d_5 was added directly to plant cell walls in an NMR tube to obtain a gel (Kim et al., 2008; Kim and Ralph, 2010). Although cellulose will not completely dissolve in these latter systems, 2D NMR of these gels allows a rapid analysis of cell wall lignin chemistry. Table 4 displays the chemical shift assignments for native lignin and other phenolic structures found in plant cell walls.

One of the many advantages of the adiabatic pulse sequence used during HSQC acquisition is its *J*-independence, allowing for quantitative measurements (Kupče and Freeman, 2007). One common quantification strategy uses the lignin methoxyl (OMe) as an internal standard. For example, the absolute content of β–O–4, β–β, and β–5 substructures can be quantified with the combination of the iodometrically determined OMe (Chen, 1992) and adiabatic HSQC NMR. The method initially determines the lignin methoxyl content iodometrically to obtain a molar quantity of OMe per g original plant material. Then, the HSQC contour integral for the Cα/Hα correlation of each lignin substructure is obtained, based upon the OMe contour integral. By knowing the iodometrically determined OMe content, the absolute molar quantity of each substructure can be obtained (Yelle et al., 2008b, 2011).

4.5 X-ray Photoelectron Spectroscopy (XPS)

XPS is a surface analysis technique that can give the elements and types of bonds present at the surface. XPS analysis involves the beaming of a photon to a sample. According to Einstein's photoelectric effect, an electron is emitted from the surface. The binding energy (E_b) of this electron is recorded and analyzed. Each element has a characteristic E_b. Therefore, XPS can be used to ascertain surface elemental composition. It also provides information about the chemical surface with a spatial resolution of a few millimeters and a depth resolution of 5 nm, depending on the takeoff angle (Kamdem et al., 1991).

Different scan resolutions yield different information. A survey scan will give the elements present at the surface. A low-resolution scan gives the percentage of each element present, the atomic concentrations are calculated through their peak intensities. Elements important in the study of lignin include carbon (C_{1s}), oxygen (O_{1s}), nitrogen (N_{1s}), sodium (Na_{1s}), and sulfur (S_{2s} and S_{2p}). A high-resolution scan gives the types of bonds and concentrations present, each peak shifts depending on which atoms the analyzed atom is bound to. For example, in the case of carbon (C_{1s}), the high-resolution spectra may consist of four component peaks around 285.0, 286.9, 288.7, and 289.3 eV. These subpeaks correspond to C_1 (C–C or C–H), C_2 (C–OH or C–O–C), C_3 (O–C–O or C=O), and C_4

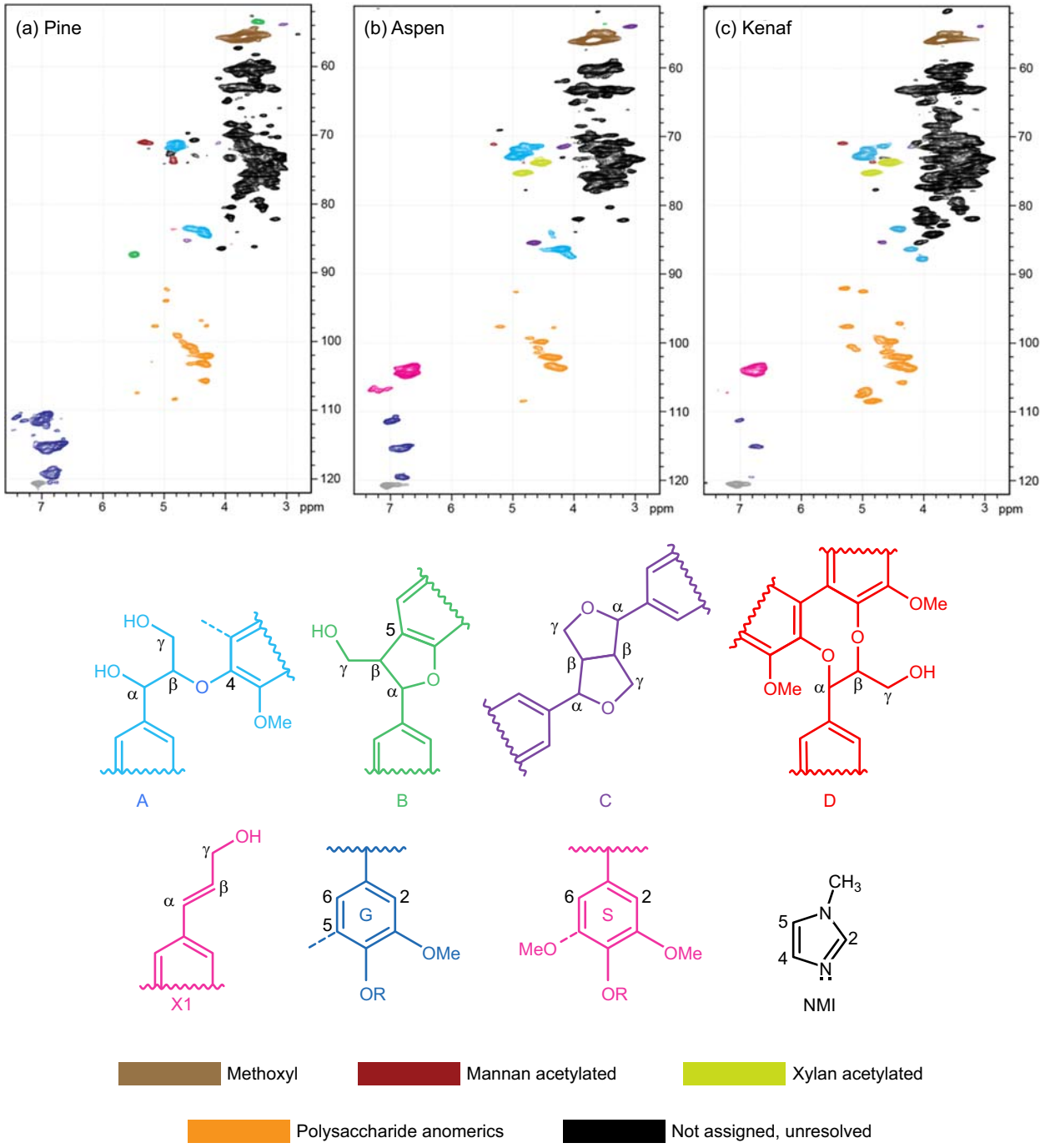

Figure 11 Two-dimensional $^{1}H-^{13}C$ correlation HSQC NMR spectra from nonderivatized plant cell walls: (a) pine, (b) aspen, and (c) kenaf at 500 MHz. Note that these spectra cover the range for all the cell wall components—cellulose, hemicelluloses, and lignin. All contour colors can be matched to their respective structure: (A) β-aryl ether in cyan (lighter gray in print versions), (B) phenylcoumaran in green (light gray in print versions), (C) resinol in purple (black in print versions), (D) dibenzodioxocin in red (gray in print versions), (X1) cinnamyl alcohol endgroups in magenta (dark gray in print versions), (G) guaiacyl in dark blue (darkest gray in print versions), (S) syringyl in fuchsia (darker gray in print versions), and (NMI) 1-methylimidazole in gray. Other structures include: lignin methoxyl in brown, H–2/C–2 and H–3/C–3 correlations for the acetylated structure of β–D–Man*p*^{I} in maroon, H–2/C–2 and H–3/C–3 correlations for the acetylated structure of β–D–Xyl*p*^{I} in chartreuse, polysaccharide anomerics in orange, and structures currently not assigned or unresolved in black.

Table 4 NMR Chemical Shift Assignments (ppm) for Native Lignin and Phenolics found in Plant Cell Walls in DMSO-*d*6/pyridine-*d*5 (4:1). **A–H/G**, β–O–4-H/G; **A–S**, β–O–4–S; **B**, β–5; **C**, β–β; **D**, dibenzodioxocine (5–5/4–O–β); **SD**, spirodienone (β–1); **X1**, cinnamyl alcohol end group; **G**, guaiacyl; **G′**, guaiacyl (oxidized α-ketone); **S**, syringyl; **S′**, syringyl (oxidized α-ketone); **H**, *p*-hydroxyphenyl; **PB**, *p*-hydroxybenzoates; **FA**, ferulate; ***p*CA**; *p*-coumarates

	α(7)	β(8)	γ(9)	2	3	5	6
A–H/G	71.3/4.87	84.4/4.39 *threo*	60.1/3.73				
		83.9/4/45 *erythro*	60.1/3.40				
A-S	71.3/4.87	87.2/4.09 *threo*	60.1/3.73				
		86.2/4.22 *erythro*	60.1/3.40				
A–γ–Ac			63.3/4.42				
			63.3/3.94				
B	87.1/5.55	54.3/3.97	62.8/3.80				
C	85.0/4.67	53.7/3.06	71.0/4.14				
			71.0/3.77				
D	83.4/4.97	85.7/3.97					
SD	81.2/5.13	60.2/2.82 β					
		79.7/4.20 β'					
X1	128.5/6.49	128.7/6.38	61.7/4.15				
G				110.8/7.02		115.2/6.90	115.2/6.90
						119.0/6.87	119.0/6.87
G′				111.3/7.52			122.9/7.57
S				103.7/6.73			103.7/6.73
S′				106.7/7.24			106.7/7.24
H				127.9/7.27			127.9/7.27
PB				131.4/7.71			131.4/7.71
FA	144.9/7.53	115.6/6.39		111.1/7.36			123.4/7.14
*p*CA	144.9/7.53	113.9/6.29		130.2/7.49	115.8/6.84	115.8/6.84	130.2/7.49

Adapted from Kim and Ralph (2010).

(O—C═O), respectively (Kamdem et al., 1991). A disadvantage of XPS is that it cannot detect H. This may lead to problems in differentiating a carboxylic acid from an ester, for example. Nevertheless, XPS is straightforward, easy to use, and nondestructive, which partly accounts for its extensive use in recent years.

In studying lignin, XPS is most often used to confirm and compare modifications, rather than determine the chemical structure. For example, XPS has been used to determine the effect of plasma modification on lignin (Zhou et al., 2012). Low-resolution XPS spectra gave an O/C atomic ratio of 0.25 for untreated lignin and 0.40 after oxygen plasma treatment, confirming surface oxidation. High-resolution XPS spectra showed an increase of 126%, 37%, and 246% in oxidized carbons, C_2, C_3, and C_4, respectively (Zhou et al., 2012). Other examples using XPS for characterizing lignin modification include investigating the

Table 5 Differential Scanning Calorimetry Results for Select Lignin Types

Lignin Type	T_g (°C)	ΔC_p (J/g°C)
Alcell	108	0.403
Pine	107	0.417
Bagasse	116	0.386
Eucalyptus	136	0.182
Aspen	162	0.102
Aspen	89.9	0.230
Mixed oak	174	0.141
Mixed oak	96.9	0.282
Mixed oak	106	0.250
Tulip poplar	119	0.315
Tulip poplar	127	0.206
Tulip poplar	141	0.078
Switchgrass	121	0.239
Black locust	105	0.248
Corn stover	131	0.060
Newsprint	140	0.105

Adapted from Sammons et al. (2013).

adsorption of laccases on lignin by following the N_{1s} peak (Saarinen et al., 2009) and determining the concentration of lignin on lignin-based electrospun nanofibers by following the S_{2p} peak (Ago et al., 2012).

5. Thermal Properties

Techniques used for determining thermal properties of polymers are also routinely applied to determine the thermal properties of lignin. DSC is a thermoanalytical technique during which the temperature of a sample and reference material is increased at a constant rate. The heat flow required to increase the temperature of the sample and the reference material at a constant rate is measured. The technique is used for determining phase transitions, relying on the principle that, as the sample undergoes a phase transition more or less heat will need to flow to it than to the reference to maintain both at the same temperature. Often the glass transition temperature (T_g) and the change in heat capacity (ΔC_p) are reported. DSC results for select lignin types are summarized in Table 5. The differences, even within species are typical and can be due to differences in lignin preparations. Variations in T_g and ΔC_p can be correlated to variations in chemical structure (Sammons et al., 2013).

TGA is another thermoanalytical technique in which changes in the mass of a sample is reported as a function of increasing temperature at a constant heating rate (dynamically) or as a function of time (isothermally). In the study of lignin, TGA is primarily conducted dynamically and provides information about degradation temperatures and other phase transition temperatures. Figure 12 shows the TGA and derivative thermogravimetric analysis

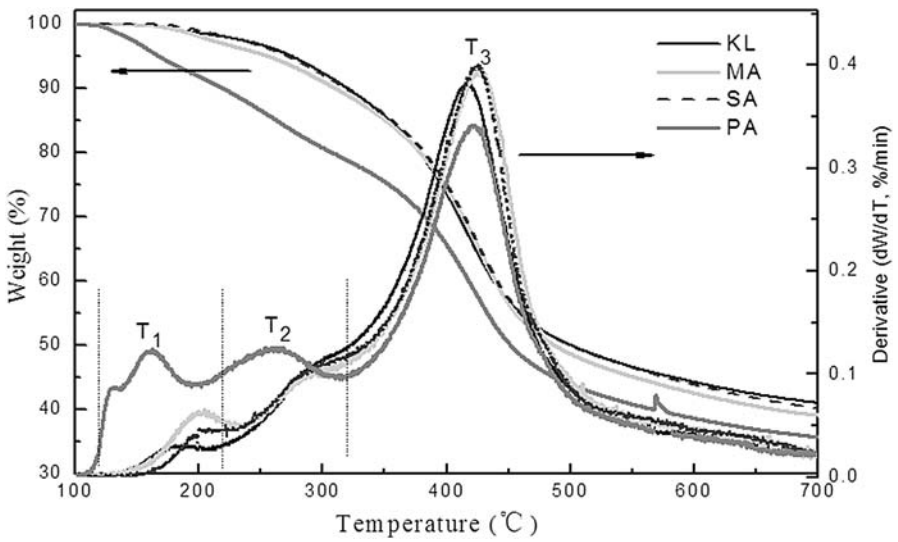

Figure 12 Thermogravimetric analysis curves for unmodified kraft lignin (KL) from ponderosa pine, and for KL modified with maleic anhydride (MA), succinic anhydride (SA), and phthalic anhydride (PA) (Chen et al., 2014).

Table 6 Thermogravimetric Analysis (TGA) and Derivative Thermogravimetric Analysis (DTGA) Curves for Unmodified Kraft Lignin (KL) and KL Modified with Maleic Anhydride (MA), Succinic Anhydride (SA), and Phthalic Anhydride (PA)

Lignin Type	T_0 (°C)	T_1 (°C)	T_2 (°C)	T_3 (°C)
Unmodified KL	156.6	180.0	290.2	417.5
MA-KL	159.5	203.3	292.6	427.0
SA-KL	170.4	220.9	298.7	425.7
PA-KL	122.8	160.6	258.8	420.0

Adapted from Chen et al. (2014).

(DTGA) curves of a specific KL and KL modified in esterification reactions. The DTGA curve more easily shows three degradation temperatures, T_1, T_2, and T_3 and the onset temperature T_0 (Table 6). In this case, modifying the lignin with succinic anhydride resulted in a lignin that was more thermally stable than the others, suggesting that it could be processed at higher temperatures in lignin-based composites (Chen et al., 2014). Combining TGA with mass spectroscopy, TGA/MS, allows for the characterization of the gaseous products of lignins that are a result of thermal degradation. TG/MS results indicate that water and gaseous products represent about 2/3 of volatiles during degradation while monomers and oligomers amount to 1/3 (Jakab et al., 1997). Furthermore, differences in lignins are apparent. Softwood lignins (guaiacyl) produce the highest char yield, whereas hardwood lignins (guaiacyl and syringyl) yield the lowest amount of char. The conclusion is that guaiacyl units are more prone to thermally initiated condensation reactions than syringyl units (Jakab et al., 1997).

6. Mechanical Properties

As a polymer, lignin has viscoelastic properties. DMA is a technique used to characterize viscoelasticity. During this test, a sinusoidal stress is applied to a sample and the strain is measured. If the sample is purely elastic, the strain will be perfectly in phase with the applied stress. If the sample is purely viscous, there will be a 90° phase lag in strain compared with the applied stress. Viscoelastic polymers such as lignin exhibit both viscous and elastic characteristics. DMA testing reports the storage modulus (E′, a result of elastic properties), loss modulus (E″, a result of viscous properties), and the ratio between the two (E″/E′) known as tan δ where δ is the phase lag between stress and strain. DMA is most often performed with the frequency constant and the temperature changed at a constant rate. This mode allows for the identification of the glass transition temperature and other transitions.

DMA is typically performed on solid samples. However, it can be performed on powders with some caveats. Because the calculations of E′ and E″ are dependent upon the surface area that the stress is applied, and this is unknown for powdered samples, the quantitative values are not accurate. However, the trends in changes in E′ and E″ with temperature can give useful information. In addition, because tan δ is a ratio this can still provide information about molecular transitions. Figure 13 shows the results of a DMA test that was performed on powdered KL from ponderosa pine. One can see that as the temperature increases, the storage modulus, E′, decreases with a steep decrease between 125 and 175 °C. The transitions were at around 158 and 177 °C (tan δ curve).

It is more common to perform DMA on lignin indirectly as a component of other systems. In wood, lignin is a viscoelastic component. Studies of lignin as a component of wood using DMA can be used to

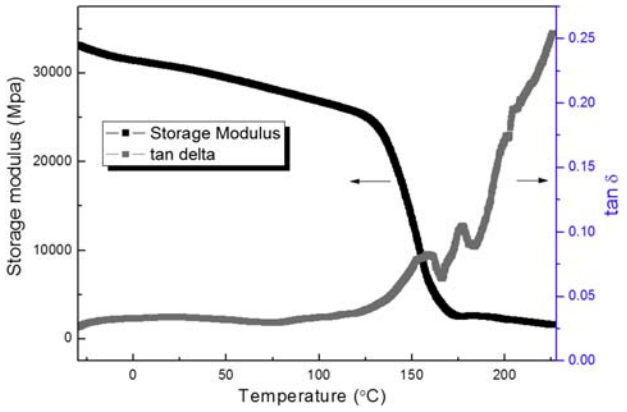

Figure 13 Dynamic mechanical analysis results from powdered kraft lignin.

correlate properties back to the lignin chemical structure. For example, using DMA it was found that a reduction in lignin content in aspen decreased the glass transition temperature, but the syringyl/guaiacyl ratio did not change it (Horvath et al., 2011). These results were used to contradict arguments that a high amount of methoxyl groups should decrease lignin glass transition temperature. DMA is also routinely used to study lignin as a component of composites.

7. Sources of Further Information

This chapter provides an introduction to common, nondegradative techniques used to characterize lignin. The discussion of each technique provides only a basic introduction to the method as well as an example as to how it is applied to lignin. Fortunately, there are many sources of further information which cover each of these techniques. The following three books are highly recommended.

1. Wood and cellulosic chemistry (Hon and Shiraishi, 2001).

   There are two chapters that are particularly useful. The first chapter covers lignin chemistry and structure, spectroscopic methods, and the structural elements in lignin and lignin degradation (Sakakibara and Sano, 2001). The second chapter covers the chemical characterization of wood and includes lignin as a component of wood. This chapter includes chemical characterization methods of lignin that are degradative, as well as chemical structure degradation methods (Baeza and Freer, 2001).

2. Methods in lignin chemistry (Lin and Dence, 1992).

   The chemical structure of lignin is explained in great detail in this book, including differences in commercial lignins, isolation of lignin, and lignin sources. As related to this chapter, this book also provides more information on many of the characterization techniques here, including lignin in the solid state characterized by FTIR spectroscopy (Faix, 1992), NMR spectroscopy (Leary and Newman, 1992), Raman spectroscopy (Atalla et al., 1992), thermal analysis (Hatakeyama, 1992), and lignin in solution characterized by UV spectroscopy (Lin, 1992).

3. Lignin and lignans (Heitner et al., 2010).

   This book delves into the chemistry of lignin, and there are two chapters that are useful in covering spectroscopic characterization methods in great detail. The first chapter covers vibrational spectroscopy and includes discussions on FTIR spectroscopy and Raman spectroscopy (Agarwal and Atalla, 2010). The second chapter is a comprehensive discussion of NMR spectroscopy as applied to lignin (Ralph and Landucci, 2010).

   It would be impossible to summarize the properties of lignin determined using the characterization techniques described in this chapter. Not only has this research been ongoing for many years, but lignin characterization and modification continue to be an active area of research. In addition, results are dependent upon the type, source, and isolation of lignin. A literature search of any of these techniques combined with lignin will yield hundreds, if not thousands, of research articles. Research articles published in peer-reviewed journals are a great source of information, particularly to obtain the most recent research results and application of these techniques to lignin characterization. The following two Web sites are particularly useful.

   a. http://www.ncsu.edu/bioresources

   This is the Web site for the online journal BioResources. It is a peer-reviewed journal that is open sources and dedicated to publishing research articles covering lignocellulosics.

   b. http://www.treesearch.fs.fed.us/

   This Web site links to the search engine, Treesearch. It will search research articles published by the USDA Forest Service. The majority of publications on Treesearch will be available to be viewed in pdf format.

Finally, there are a number of professional societies that cover lignin research. The American Chemical Society, Society of Wood Science and Technology, and the Forest Products Society all offer research articles covering lignin. The American Chemical Society is also very active in the publication of books covering the topic.

References

Agarwal, U.P., Reiner, R.S., 2009. Near-IR surface-enhanced Raman spectrum of lignin. Journal of Raman Spectroscopy 40 (11), 1527−1534.

Agarwal, U.P., Atalla, R.H., 2010. Vibrational spectroscopy. In: Heitner, C., Dimmel, D.R., Schmidt, J.A. (Eds.), Lignin and Lignans, Advances in Chemistry. CRC Press, Boca Raton, FL, pp. 103−136.

Agarwal, U.P., Ralph, S.A., 1997. FT-Raman spectroscopy of wood: identifying contributions of lignin and carbohydrate polymers in the spectrum of black spruce (*Picea mariana*). Applied Spectroscopy 51, 1648−1655.

Ago, M., Jakes, J.E., Johansson, L.-S., Park, S., Rojas, O.J., 2012. Interfacial properties of lignin-based electrospun nanofibers and films reinforced with cellulose nanocrystals. Applied Materials and Interfaces 4, 6849−6856.

Atalla, R.H., Agarwal, U.P., Bond, J.S., 1992. Raman spectroscopy. In: Lin, S.Y., Dence, C.W. (Eds.), Methods in Lignin Chemistry. Springer-Verlag, Berlin, pp. 465−472.

Baeza, J., Freer, J., 2001. Chemical characterization of wood and its components. In: Hon, D.N.-S., Shiraishi, N. (Eds.), Wood and Cellulosic Chemistry, second ed. Marcel Dekker, Inc., New York, NY, pp. 275−384.

Boerjan, W., Ralph, J., Baucher, M., 2003. Lignin biosynthesis. Annual Review Plant Biology 54, 519−546.

Chen, C.L., 1992. Determination of methoxyl groups. In: Lin, S.Y., Dence, C.W. (Eds.), Methods in Lignin Chemistry. Springer-Verlag, Berlin, pp. 83−109.

Chen, Y., Stark, N.M., Cai, Z., Frihart, C.R., Lorenz, L.F., Ibach, R.E., 2014. Chemical modification of kraft lignin: effect on chemical and thermal properties. Bioresources 9 (3), 5488−5500.

Ehlting, J., Mattheus, N., Aeschliman, D.S., Li, E., Hamberger, B., Cullis, I.F., Zhuang, J., Kaneda, M., Mansfield, S.D., Samuels, L., et al., 2005. Global transcript profiling of primary stems from *Arabidopsis thaliana* identified candidate genes for missing links in lignin biosynthesis and transcriptional regulators of fiber differentiation. The Plant Journal 42, 618−640.

Faix, O., 1992. Fourier transform infrared spectroscopy. In: Lin, S.Y., Dence, C.W. (Eds.), Methods in Lignin Chemistry. Springer-Verlag, Berlin, pp. 83−109.

Fengel, D., Wegener, G., 1983. Wood. Walter de Gruyter, New York.

Freeman, S.K., 1974. Applications of Laser Raman Spectroscopy. John Wiley, New York.

Fujimoto, A., Matsumoto, Y., Chang, H.M., Meshitsuka, G., 2005. Quantitative evaluation of milling effects on lignin structure during the isolation process of milled wood lignin. Journal of Wood Science 51, 89−91.

Goldschmid, O., 1954. Determination of phenolic hydroxyl content of lignin preparations by ultraviolet spectrophotometry. Analytical Chemistry 26 (9), 1421−1423.

Hatakeyama, H., 1992. Thermal analysis. In: Lin, S.Y., Dence, C.W. (Eds.), Methods in Lignin Chemistry. Springer-Verlag, Berlin, pp. 200−214.

Heitner, C., Dimmel, D., Schmidt, J. (Eds.), 2010. Lignin and Lignans: Advances in Chemistry. CRC Press, Boca Raton, FL.

Hendra, P.J., Jones, C., Warnes, G., 1991. FT-Raman Spectroscopy. Ellis-Horwood, Chicester, UK.

Hon, D.N.-S., Shiraishi, N. (Eds.), 2001. Wood and Cellulosic Chemistry. Marcel Dekker, New York.

Horvath, B., Peralta, P., Frazier, C., Peszlen, I., 2011. Thermal softening of transgenic Aspen. Bioresources 6 (2), 2125−2134.

Ikeda, T., Holtman, K., Kadla, J.F., Chang, H.M., Jameel, H., 2002. Studies on the effect of ball milling on lignin structure using a modified DFRC method. Journal of Agricultural and Food Chemistry 50 (1), 129−135.

Jakab, E., Faix, O., Till, F., 1997. Thermal decomposition of milled wood lignins studied by thermogravimetry/mass spectrometry. Journal of Analytical and Applied Pyrolysis 40-41, 171−186.

Kamdem, D.P., Riedl, B., Adnot, A., Kaliaguine, S., 1991. ESCA spectroscopy of poly (methyl methacrylate) grafted onto wood fibers. Journal of Applied Polymer Science 43 (10), 1901−1912.

Kim, H., Ralph, J., Akiyama, T., 2008. Solution-state 2D NMR of ball-milled plant cell wall gels in DMSO-d_6. Bioenergy Research 1, 56−66.

Kim, H., Ralph, J., 2010. Solution-state 2D NMR of ball-milled plant cell wall gels in DMSO-d_6/pyridine-d_5. Organic and Biomolecular Chemistry 8 (3), 576−591.

Kupče, E., Freeman, R., 2007. Compensated adiabatic inversion pulses: broadband INEPT and HSQC. Journal of Magnetic Resonance 187, 258−265.

Lai, Y.Z., Sarkanen, K.V., 1971. Isolation and structural studies. In: Sarkanen, K.V., Ludwig, C.H. (Eds.), Lignins: Occurrence, Formation, Structure and Reactions. Wiley Interscience, New York, pp. 165−240.

Leary, G.J., Newman, R.H., 1992. Cross polarization/magic angle spinning nuclear magnetic resonance (CP/MAS NMR) spectroscopy. In: Lin, S.Y., Dence, C.W. (Eds.), Methods in Lignin Chemistry. Springer-Verlag, Berlin, pp. 146−161.

Lin, S.Y., 1992. Ultraviolet spectroscopy. In: Lin, S.Y., Dence, C.W. (Eds.), Methods in Lignin Chemistry. Springer-Verlag, Berlin, pp. 215−232.

Lin, S.Y., Dence, C.W. (Eds.), 1992. Methods in Lignin Chemistry. Springer-Verlag, Berlin.

Long, D.A., 1977. Raman Spectroscopy. McGraw Hill, New York.

Lu, F., Ralph, J., 2003. Non-degradative dissolution and acetylation of ball-milled plant cell walls: high-resolution solution state NMR. The Plant Journal 35 (4), 535−544.

Ralph, J., Landucci, L.L., 2010. NMR of Lignins. In: Heitner, C., Dimmel, D.R., Schmidt, J.A. (Eds.), Lignin and Lignans, Advances in Chemistry. CRC Press, Boca Raton, FL, pp. 137−244.

Sakakibara, A., Sano, Y., 2001. Chemistry of lignin. In: Hon, D.N.-S., Shiraishi, N. (Eds.), Wood and Cellulosic Chemistry, second ed. Marcel Dekker, Inc., New York, NY, pp. 109−173.

Saarinen, T., Orelma, H., Grönqvist, S., Andberg, M., Holappa, S., Laine, J., 2009. Adsorption of different laccases on cellulose and lignin surfaces. Bioresources 4 (1), 94−110.

Sammons, R.J., Harper, D.P., Labbé, N., Bozell, J.J., Elder, T., Rials, T.G., 2013. Characterization of organosolv lignins using thermal and FT-IR spectroscopic analysis. Bioresources 8 (2), 2752−2767.

Vanholme, R., Demedts, B., Morreel, K., Ralph, J., Boerjan, W., 2010. Lignin biosynthesis and structure. Plant Physiology 153, 895−905.

Wegener, G., Przyklenk, M., Fengel, D., 1983. Hexafluoropropanol as valuable solvent for lignin in UV and IR spectroscopy. Holzforschung 37, 303−307.

Yelle, D.J., Ralph, J., Frihart, C.R., 2008a. Characterization of nonderivatized plant cell walls using high-resolution solution-state NMR spectroscopy. Magnetic Resonance in Chemistry 46, 508−517.

Yelle, D.J., Ralph, J., Lu, F., Hammel, K.E., 2008b. Evidence for cleavage of lignin by a brown rot basidiomycete. Environmental Microbiology 10 (7), 1844−1849.

Yelle, D.J., Wei, D.S., Ralph, J., Hammel, K.M., 2011. Multidimensional NMR analysis reveals truncated lignin structures in wood decayed by the brown rot basidiomycete *Postia placenta*. Environmental Microbiology 13 (4), 1091−1100.

Zhou, X., Zheng, F., Liu, X., Tang, L., Xue, G., Du, G., Yong, Q., Chen, M., Zhu, L., 2012. Glass transition of oxygen plasma treated enzymatic hydrolysis lignin. Bioresources 7 (4), 4776−4785.

ELSEVIER

LIGNIN IN POLYMER COMPOSITES

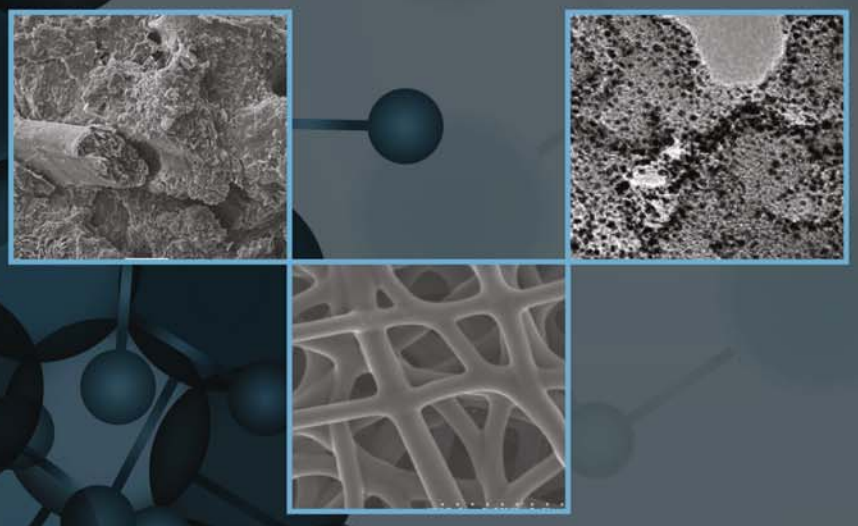

EDITED BY:
OMAR FARUK
MOHINI SAIN

LIGNIN IN POLYMER COMPOSITES

Omar Faruk

Mohini Sain

ELSEVIER

Amsterdam • Boston • Heidelberg • London • New York • Oxford
Paris • San Diego • San Francisco • Singapore • Sydney • Tokyo

William Andrew is an imprint of Elsevier

William Andrew is an imprint of Elsevier
The Boulevard, Langford Lane, Kidlington, Oxford, OX5 1GB, UK
225 Wyman Street, Waltham, MA 02451, USA

Notices
Knowledge and best practice in this field are constantly changing. As new research and experience broaden our understanding, changes in research methods, professional practices, or medical treatment may become necessary.

Practitioners and researchers must always rely on their own experience and knowledge in evaluating and using any information, methods, compounds, or experiments described herein. In using such information or methods they should be mindful of their own safety and the safety of others, including parties for whom they have a professional responsibility.

To the fullest extent of the law, neither the Publisher nor the authors, contributors, or editors, assume any liability for any injury and/or damage to persons or property as a matter of products liability, negligence or otherwise, or from any use or operation of any methods, products, instructions, or ideas contained in the material herein.

ISBN: 978-0-323-35565-0

British Library Cataloguing-in-Publication Data
A catalogue record for this book is available from the British Library

Library of Congress Cataloging-in-Publication Data
A catalog record for this book is available from the Library of Congress

Publisher: Matthew Deans
Acquisition Editor: David Jackson
Editorial Project Manager: Peter Gane
Production Project Manager: Susan Li
Designer: Mark Rogers

Typeset by TNQ Books and Journals
www.tnq.co.in

Printed and bound in the United States of America